Organic & Biomolecular Chemistry

RSC Publishing

PAPER

View Article Online
View Journal | View Issue

A new family of bioorthogonally applicable fluorogenic labels†‡

Cite this: *Org. Biomol. Chem.*, 2013, **11**, 3297

András Herner,[a] Ivana Nikić,[b] Mihály Kállay,[c] Edward A. Lemke[b] and Péter Kele*[a]

Received 7th November 2012,
Accepted 5th March 2013

DOI: 10.1039/c3ob40296g

www.rsc.org/obc

Synthetic procedures for the construction of fluorogenic azido-labels were developed. Photophysical properties were elaborated by experimental and theoretical investigations. Of the newly synthesized fluorogenic and bioorthogonally applicable dyes two were selected on the basis of their fluorogenic performance and further subjected to *in vitro* and *in vivo* studies. Both tags exhibited excellent fluorogenic properties as in aqueous medium, the azide form of the selected dyes is virtually non-fluorescent, while their "clicked" triazole congeners showed intense fluorescence. One of these labels showed a very large Stokes shift. To the best of our knowledge this is the first reported case of mega-Stokes type of fluorogenic labels. These studies have justified that these two fluorogenic tags are remarkably suitable for bioorthogonal tagging schemes. The developed synthetic approach together with the theoretical screen of possible fluorogenic tags will enable the generation of libraries of such tags in the future.

Introduction

Small molecular modulation of biomatter is of great importance in modern chemical biological research. The development of bioorthogonal chemistry schemes has greatly facilitated the exploration of biochemical processes. Continuous efforts have been made lately for the development of new bioorthogonal reagents that offer selective, often site-specific, and high-yielding reactions with biological targets. Up to now, these efforts have resulted in the development of several bioorthogonal reagents *e.g.* (cyclo)alkynes, azides or tetrazines.[1] Non-natural biomolecular building blocks containing one or more of these bioorthogonal functions offer easy and specific incorporation of these chemical reporters into target structures by taking advantage of gene technology or the metabolic machinery of living organisms.[2] Of the biomolecular labeling techniques fluorescent modification of biological matter is by far the most popular one. Its popularity can be owed to the highly sensitive and relatively cheap detectability of the fluorescent signal with remarkable spatial and temporal resolution and their potential for multichannel imaging. Indeed, labeling of amino acids, proteins, lipids, nucleic acids, sugars, or even cells and viruses with synthetic fluorescent dyes has become an indispensible tool in bioanalytical sciences.[3]

One advantage of applying synthetic fluorophores is the ability to employ chemical approaches to control the photophysical properties and chemical reactivity of fluorescent tags. Applying modern synthetic organic chemistry strategies enables efficient tailoring of the chemical structure to obtain probes for specific needs. Fluorescence tagging schemes often follow a two (or more)-step procedure, where excessive amounts of the fluorophore are administered to the sample to be labeled. After the incubation time the unreacted reagent should be removed. However, this task is not easy in many instances and the remaining, non-specifically bound fluorescent labels contribute to very high levels of background fluorescence therefore compromising the sensitivity of detection (low signal-to-noise ratio). Solution to this problem is offered by the use of so-called fluorogenic (switchable, "turn-on") probes where the reagents are weakly or non-fluorescent at the wavelength of detection.[4] The fact that these labels are introduced as virtually non-fluorescent derivatives eliminates the need for the separation of excessive reagents without compromising sensitivity. Many fluorogenic dyes have been developed to sense for example differences in microenvironments, however, very few fluorogenic reagents are available for covalent modification of biomatter.[4,5]

Bioorthogonal tagging schemes have benefited greatly from the use of the azide group. The significance of this functional group lies behind its high energetic feature together with its

[a]*Institute of Chemistry, Eötvös Loránd University, H-1117, Pázmány Péter sétány 1a, Budapest, Hungary. E-mail: kelep@elte.hu; Fax: (+36)1 372 2909; Tel: (+36)1 209 0555 ext. 1610*
[b]*Structural and Computational Biology Unit, EMBL, Meyerhofstrasse 1, D-69117 Heidelberg, Germany*
[c]*Department of Physical Chemistry and Materials Science, Budapest University of Technology and Economics, P. O. Box 91, H-1521, Budapest, Hungary*

†This work is dedicated to Roger M. Leblanc on the occasion of his birthday.

‡Electronic supplementary information (ESI) available: ^{1}H- and ^{13}C-NMR spectra for small molecules and fluorescence spectra for **1a–c** and **9a–c**, further images of live cell labeling experiments and optimized geometries are provided. See DOI: 10.1039/c3ob40296g

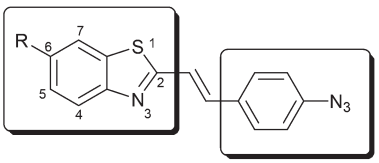

Fig. 1 Modular setup of fluorogenic tags.

stability under a wide variety of reaction conditions.[6] Noteworthy is its selective reactivity that enables reactions solely with particular counterparts in the presence of several other functional groups present in biological media. Its participation in conventional bioorthogonal modulation schemes *e.g.* copper-catalyzed or strain promoted cycloaddition with alkynes or the Staudinger ligation technique with phosphanes as reaction partners has just raised the azide group to the most popular one.[7] Another less emphasized feature of the azide group is the fact that its incorporation into fluorescent scaffolds often results in dramatic drop in fluorescence intensity. These fluorogenic compounds remain non-fluorescent as long as the azide function is intact. They become intensely fluorescent, however, when the azide group is converted into a different functionality. Examples show that conversion of azides into amines or triazoles results in changes in the electronic system and the originally quenched fluorescence reinstates.[4,5] Quite simply, the azide moiety offers a bioorthogonally applicable, switchable two-in-one combination under certain circumstances. Despite their obviously advantageous features azido quenched fluorescent tags are rarely reported. Design of fluorogenic labels mostly relies on empirical trial and error methods and very few examples use theoretical prediction of such features. Moreover, the so-far presented fluorogenic azido-tags lack the possibility of fine-tuning *e.g.* emission wavelengths, as simple fluorogenic scaffolds bear the azide moiety. Herein we introduce an approach that could be used in the design of more complex fluorogenic units with theoretically predictable photophysical features (Fig. 1).

Results and discussion

Design

We have chosen the 1,3-benzothiazole (Fig. 1) scaffold as a starting module for its appealing synthetic and fluorescent features. 1,3-Benzothiazoles are easily modified at their 2nd and 6th positions; therefore we have also intended to use these sites for further modifications. On the one hand we planned to shift the emission wavelength of the benzothiazole core towards the red regime by means of extending the conjugated system. On the other hand we intended to modulate the emission intensity of the fluorescent scaffold by incorporating an azide moiety into the framework. Based on former studies and theoretical investigations,[5,8] we have anticipated that incorporation of a 4-azidostyryl moiety that can either be incorporated directly or in the form of its nitro-precursor will satisfy both needs. We will show that position 6 is suitable for tuning the spectral parameters by incorporating electron donating (methoxy) or withdrawing (nitro) groups. Based on our earlier work with polymethine-fluorophores we also hoped that some of these dyes will exhibit large Stokes shifts in their fluorescent form.[9]

Synthesis

Commercially available benzothiazole scaffolds **2a** and **2b** were condensed with 4-nitrobenzaldehyde in molten *p*-TsOH in a minimum amount of refluxing toluene providing exclusively the *trans*-styryl products (**4a–b**) in moderate to good yields (Scheme 1, Method A). Reduction of the nitro-group with tin(II) chloride under acidic conditions and subsequent diazotization based azide group incorporation resulted in fluorogenic dyes **1a–b** in medium yields. In the case of 2-methyl-6-nitro-1,3-benzothiazole this reaction route was not applicable for **2c** bearing two nitro groups. **2c** was therefore reacted with 4-azidobenzaldehyde (**6**) in DMSO at r.t. in the presence of NaOMe giving rise to **7c** in medium yield. This intermediate was then subjected to acid catalyzed elimination effected by TFA to obtain fluorogenic dye **1c** in moderate yield (Scheme 1, Method B). Method B was found to be less efficient for the synthesis of **1a** as it gave a much lower overall yield (6%). This method was also not suitable for the production of **1b** as it resulted in a mixture of products in low yields.

The conditions of the elimination step in Method B were found to be strongly dependent on the nature of the substituents. For example, **1a** and **1c** were not formed when the basic medium was applied (NaOMe-DMSO at r.t.) to **7a** and **7c**. Products in these cases were only formed under acid catalyzed conditions. On the other hand, the electron-donating methoxy substituent facilitated the base catalyzed elimination step but resulted in an inseparable mixture of products. It is noteworthy to mention that in the case of Method B when the addition–elimination steps were carried out in a sequential manner, separation and the purification of the desired products were greatly facilitated by the intermediate primer adduct (**7**).

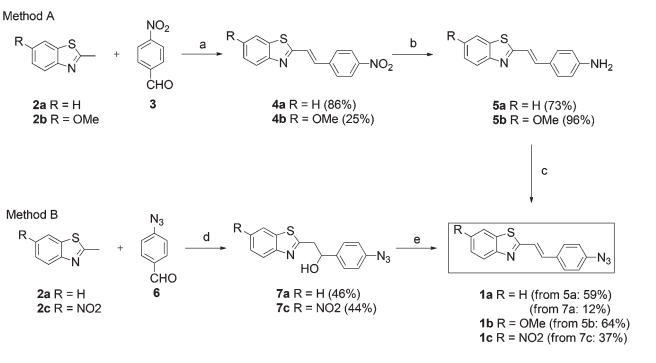

Scheme 1 Synthesis of fluorogenic dyes. (a) 1.1 eq. *p*-TsOH × H_2O, toluene, 110 °C, 18 h; (b) 5 eq. Sn(II)Cl_2 × $2H_2O$, ccHCl, r.t./45 °C, 5–20 h; (c) i. $NaNO_2$, ccHCl, 0 °C, ii. NaN_3, 0 °C→r.t., 3 h; (d) 1.2 eq. NaOMe, DMSO, r.t., 6–20 h; (e) catalytic TFA, 3 Å MS, toluene, 60–70 °C, 6–16 h.

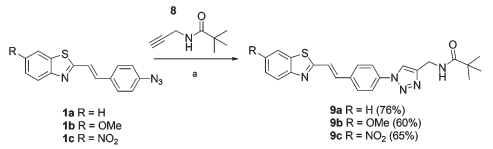

Scheme 2 (a) cat. $[Cu(PPh_3)_2]NO_3$, cat. TEA, CH_2Cl_2, r.t., 10 h.

Method A can easily be generalized and extended for a large variability of substrates for modular approaches. For example, several heterocyclic derivatives with relatively acidic methyl groups (picolynium, lepidinium, (benz)oxazoles, *etc.*) could be applied and even libraries of fluorogenic dyes become accessible in a reasonable number of synthetic steps. Work elaborating this option is currently underway in our lab and results will be reported in due course.

To our delight, all fluorogenic dyes showed very low emission intensities as a result of the quenching effect of the azide moiety. Next, we were curious, whether it is possible to turn on the fluorescence of the fluorogenic cores as a result of chemical reaction with appropriate reaction partners. Therefore we have selected *N*-(prop-2-ynyl)pivalamide probe (**8**) as a reaction partner for **1a–c** in a copper catalyzed azide–alkyne click reaction (Scheme 2).

Compound **8** was selected on the basis of not having any aromatic moieties that could affect fluorescence of the products by any means. The click reactions were performed in a dichloromethane solvent with a drop of triethylamine and a catalytic amount of Cu(I)-catalyst[10] at room temperature. Products (**9a–c**) were then collected by filtration and analyzed for their fluorescent properties.

Spectroscopic measurements

We have studied the fluorescent properties of the click-products, **9a–c**, in comparison to their parent azides, **1a–c**, in DMSO, CH_2Cl_2 and water (Table 1). In DMSO very low intensity of fluorescence was observed for all azides. Triazoles on the other hand showed orders of magnitudes stronger fluorescence, with **9b** showing the best performance. In all cases hydrogen bond formation with water decreased the fluorescence intensities (ESI‡).

In fact, in the case of **1b** and **1c** practically no fluorescence could be detected in aqueous solutions therefore the fluorescence of the corresponding triazoles (**9b**, **9c**) implies remarkable increase in the fluorescence signal (Fig. 2 and 3). These results suggest that **1b** and **1c** are particularly suitable to be applied in aqueous solutions. Excitation wavelengths were found to be very similar for all fluorogenic dyes but emission maxima were shifted towards the red regime in the order of **9a** < **9b** ≪ **9c**. Noteworthy is to mention the spectral properties of **9c**. It exhibits a large Stokes-shift (called "mega-Stokes"[10]) of 190 nm in water providing us with the possibility of more sensitive detection by eliminating the interfering scattered light and self-absorption. Moreover, to the best of our knowledge, such a combination of fluorogenic and mega-Stokes properties is unprecedented in the literature. Dyes of this kind are exceptionally useful in Förster resonance energy transfer (FRET) applications as the dye emission does not interfere with the spectral bands of the second fluorophore, which is a common problem in FRET technology.

Regarding the emission wavelengths, we observed a small but persistent blue shift in all cases for the triazoles compared to their corresponding azides. This is most likely in connection

Table 1 Photophysical properties of azides and the corresponding triazoles

Fluorophore	1a	9a	1b	9b	1c	9c
λ_{max} (abs)/nm[a]	360	368	371	368	388	355
$\varepsilon/10^4$ M^{-1} cm^{-1}[a,b]	4.00	5.30	3.60	4.22	3.21	2.27
λ_{max} (exc)/nm[a]	362	346	357	361	392	385
λ_{max} (em)/nm[a]	455	417	446	445	586	530
Stokes-shift/nm[a]	93	71	89	84	194	145
Φ_F [a,d]	0.001	0.045	0.002	0.439	0.047	0.068
Φ_F (triazole)/Φ_F (azide)[a]	45		220		1.5	
λ_{max} (exc)/nm[c]	350	343	352	352	390	381
λ_{max} (em)/nm[c]	410	414	427	437	522	489
λ_{max} (exc)/nm[e]	n.d.[f]	335	357	355	n.d.[f]	350
λ_{max} (em)/nm[e]	n.d.[f]	421	455	453	n.d.[f]	540
Stokes-shift/nm[e]	n.d.[f]	86	98	98	n.d.[f]	190

[a] In DMSO. [b] Measured at λ_{max} (abs). [c] In CH_2Cl_2. [d] Relative to quinine sulfate in 0.5 M H_2SO_4.[11] [e] In water. [f] Not detectable, in the background.

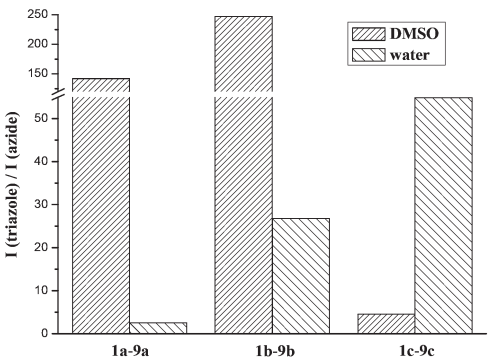

Fig. 2 Enhancement of fluorescence intensity at λ_{max} (em) of the triazoles in DMSO and water solvent. The concentration of azides and the corresponding triazoles were the same.

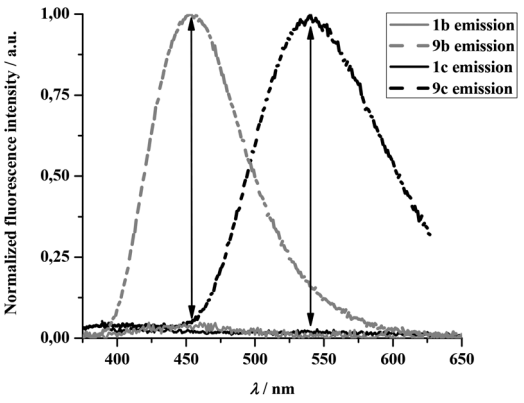

Fig. 3 Normalized emission spectra of **1b–9b** and **1c–9c**.

with the change in molecular dipole moments associated with the evolution of the triazole motif.

Quantum chemical calculations

To interpret the experimentally observed behavior of the fluorophores we performed quantum chemical calculations using the Gaussian 09 package.[12] To accelerate the calculations we employed propyne as a model system instead of the click reagent *N*-(prop-2-ynyl)pivalamide used in the experiments. The geometries for all the compounds were optimized at the density functional theory (DFT) level choosing the PBE0 functional[13,14] and the 6-311++G** basis set. All the DFT calculations were performed with dichloromethane as a solvent invoking the polarized continuum model.[15] Though the experiments were carried out in different solvents, we chose dichloromethane since the polarity of this solvent and the probability of the formation of specific solute–solvent interactions are low enabling the simplified treatment of the solvent effects. Excited-state properties were calculated using the time-dependent DFT method[16] with the same functional, basis set, and solvation model. To simulate the experimental absorption (excitation) spectra vertical excitation energies as well as oscillator strengths were calculated at the optimized ground-state geometries. For the calculation of fluorescence wavelengths and intensities the geometries of the first excited singlet state were optimized and vertical excitation energies and oscillator strengths were calculated at the minima of the excited-state surfaces.

We note that several isomers (conformers) exist for the investigated molecules. First, stereoisomerism about the central double bond can be observed. Since NMR experiments revealed that only the *trans* isomers were formed in the synthesis, we considered the latter in the calculations. Second, because of the restricted rotation about other bonds further *cis* and *trans* isomers can be identified. We calculated the energies for all the possible isomers and only retained the most stable one for each molecule for the excited-state calculations. As we tested for the H-substituted compound the excited-state properties are largely independent of which isomer is considered, thus the above restriction does not influence our conclusions.

The optimized ground-state geometries for the most stable isomers are presented (see ESI‡). The geometries are planar for the azide derivatives, while for the triazoles the triazole ring forms an angle of about 30 degrees with the plane of the phenyl ring.

We found that the rotational barrier of the rotation around the bond connecting the azide/triazole moiety to the phenyl ring is low, consequently the rotation is allowed at room temperature. Since the molecules are expected to have several low-lying excited states, and upon the rotation around a bond the excited-state potential energy surfaces (PESs) may cross each other and an internal conversion may take place, we mapped the excited-state PESs in more detail and started the geometry optimization from several initial geometries differing in the torsion angle between the azide/triazole and phenyl groups.

Table 2 Calculated transition wavelengths (λ) and oscillator strengths for the fluorophores[a]

	Absorption		Emission	
Substituent	λ/nm	Osc. strength	λ/nm	Osc. strength
Azides				
–H	393 (350)	1.76	451 (410)	1.78
–OMe	407 (352)	1.78	467 (427)	1.83
$-NO_2$	445 (390)	1.51	512 (522)	1.60
Triazoles				
–H	388 (343)	1.78	442 (414)	1.78
–OMe	402 (352)	1.71	458 (437)	1.81
$-NO_2$	422 (381)	1.58	497 (489)	1.66

[a] Numbers in parentheses show the experimental results in CH_2Cl_2.

Provided that the excited-state geometry optimization is started from a geometry close to the optimized ground-state structure, the relaxation of the geometry is moderate for all molecules, and the optimized S_1-state geometries are close to the ground-state ones. Remarkable conformational change takes place only at the triazole moiety of the triazole derivatives, which is perpendicular to the phenyl ring in the S_1 state of the unsubstituted molecule, while the excited-state conformation is planar for the other compounds. The calculated transition wavelengths and oscillator strengths are collected in Table 2.

The agreement of the experimental and theoretical absorption and emission wavelengths is satisfactory and justifies the selection of the applied theoretical model. However, the oscillator strengths for the emissions are practically identical for the azide and the triazole derivatives suggesting that for the azides the fluorescence from the minima found in the optimizations is not the dominant decay channel.

We found that upon the rotation of the azide group the first excited state interchanges with a non-emissive state. In the case the excited-state geometry optimization is started from the distorted structure, we obtain a minimum on the potential energy surface of the latter state, which is very close to the ground-state potential surface (*ca.* 0.5 eV above the ground state energy) and the transition probability of the excited state → ground state transition is zero. The corresponding geometries are displayed (see ESI‡). Consequently, these results suggest the existence of an alternative, radiationless decay channel explaining the low fluorescence intensities observed for the azide derivatives. Due to the conformation change of the azide group, a state-switch takes place which opens up the possibility of the internal conversion of the two lowest excited states followed by another internal conversion process to the ground state.

In vitro peptide labeling

Following model reactions and photophysical characterization we were curious to test the performance of our new fluorogenic labels in action. For this we have chosen a cyclooctyne (CyO) bearing peptide sequence (CyO-Gly-Pro-Leu-Gly-Val-Arg-DL-Pra-NH_2; DL-Pra = racemic propargyl-glycine) from our previous

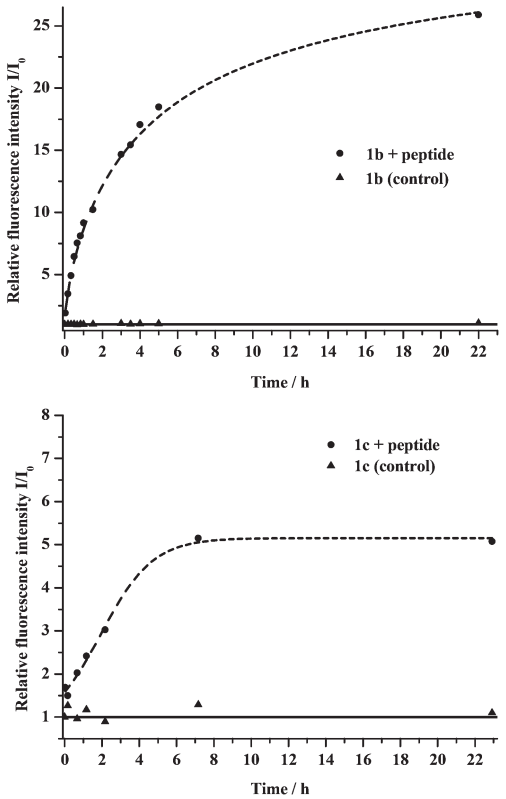

Fig. 4 Top: coupling reaction of **1b** and CyO-pep. The dots show the datapoints of the labelled peptide, the triangles belong to the control sample (without peptide). Bottom: coupling reaction of **1c** and CyO-pep. The dots show the datapoints of the labelled peptide, the triangles belong to the control sample (without peptide).

studies.[17] The cyclooctyne moiety enables rapid *in situ* copper-free tagging of the peptide *e.g.* with fluorogenic azides under physiological conditions (pH = 7.20 phosphate buffer). Due to their performance in the model reactions we have selected **1b** and **1c** for *in vitro* labeling reactions. The tagging reaction was monitored in time by following fluorescence intensity changes at 455 and 540 nm, respectively, while exciting at 355 nm. In both cases rapid increase in fluorescence intensity could be observed (Fig. 4).

Reaction with **1b** was somewhat faster than in the case of **1c**. The final fluorescence intensity was much higher for the former fluorogenic tag as well. Control reactions of both fluorogenic tags in the absence of the peptide showed no change in fluorescence intensities, implying that there are no *e.g.* nitrene involved decomposition processes that would result in fluorescent species. The fact that the non-fluorescent azides of **1b** and **1c** show very low fluorescence intensities means that the evolving signal can be detected with excellent *s*/*n* ratios, a feature greatly desired in biological tagging schemes.

In vivo protein labeling

We were also curious to explore the performance of selected fluorogenic azido-tags under *in vivo* conditions where the dyes have to stand more challenging conditions. In our previous

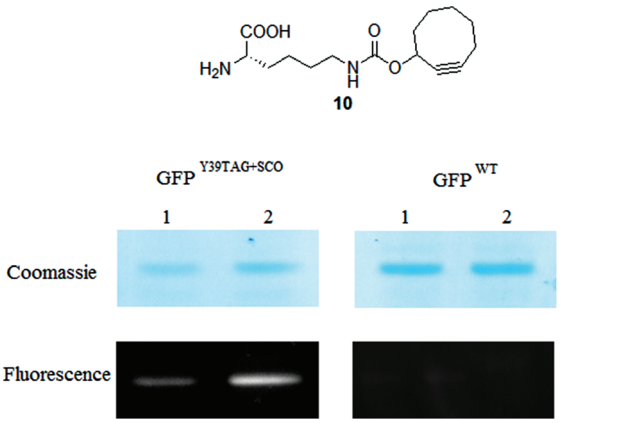

Fig. 5 Fluorescent and corresponding Coomassie stained images of GFP$^{Y39TAG+SCO}$ and GFP^{wt} labeling reactions with compounds **1b**, **1c** (lanes 1 and 2, respectively) inside live *E. coli*.

work we have genetically encoded cyclooctyne (SCO) bearing unnatural amino acid **10** using a rationally engineered tRNA^{pyl}/PylRS^{AF} pair.[2a,b] An Amber (TAG) mutated Green Fluorescent Protein (GFP) reporter construct was expressed in *E. coli* cells together with a pEvol PylRS^{AF} plasmid in the presence of **10**, leading to site-specific incorporation of SCO into GFP. Living cells were treated with **1b**, **1c** and lysed subsequently. The lysates were loaded onto an SDS PAGE gel for whole cell lysate analysis. The gel was analysed for fluorescence by exciting the samples in the UV-range (365 nm) and detecting the emission intensities. Afterwards the gels were stained with Coomassie (Fig. 5).

Analysis of the gel under UV excitation revealed that both fluorogenic labels efficiently labelled the SCO-tagged GFP. In the control experiment where wild type (WT) GFP was expressed in the cells no labeling of the protein took place. Furthermore, it was also obvious that **1b** and **1c** can stand the harsh conditions applied during lysis and no fluorescent decomposition products were formed (for full details and full gel images see ESI‡). These results served as evidence that the two new fluorogenic labels can be used in bioorthogonal fluorescent tagging schemes resulting in background fluorescence free images.

Experimental

General

Unless otherwise indicated, all starting materials were obtained from commercial suppliers (Sigma-Aldrich, Fluka, Merck, Alfa Aesar, Reanal, Molar Chemicals, Romil) and used without further purification. Dichloromethane stabilized with ethanol was used, unless otherwise mentioned. SCO was purchased from Sichem (Bremen, Germany). Tamra-azide was ordered from www.baseclick.eu. Analytical thin-layer chromatography (TLC) was performed on silica gel 60 F254 precoated aluminium TLC plates from Merck. Column chromatography was carried out with flash silica gel (0.040–0.063 mm) from

Molar Chemicals. Visualisation of TLC samples was performed with a 254/365 nm UV lamp or using aqueous $KMnO_4$ solution (1.5 g $KMnO_4$, 10 g K_2CO_3 and 1.25 ml 10 m% NaOH in 200 ml of water). The aromatic azides (**1a–c**, **6**, **7a**, **7c**) could be visualised as a yellow spot after 0.5–1 minute irradiation with a 254 nm UV lamp on a TLC plate. NMR spectra were recorded on a Bruker DRX-250 or a Varian VNMRS 600 MHz spectrometer. Chemical shifts (δ) are given in parts per million (ppm) using solvent signals as the reference. Coupling constants (J) are reported in Hertz (Hz). Splitting patterns are designated as s (singlet), d (doublet), t (triplet), qr (quadruplet), qv (quintuplet), m (multiplet), dd (doublet of a doublet), td (triplet doublet), dt (doublet triplet), br s (broad singlet). The exact masses were determined with an Agilent 6230 time-of-flight mass spectrometer. Samples were introduced by the Agilent 1260 Infinity LC system and the mass spectrometer was operated in conjunction with a JetStream source in positive/negative ion mode. All melting points were measured on a Bibby Scientific SMP10 Melting Point Apparatus and are uncorrected. IR spectra were obtained on a Bruker IFS55 spectrometer on a single-reflection diamond ATR unit. The fluorescence measurements were carried out on a Varian Cary Eclipse spectrofluorimeter, the UV-VIS measurements on a Jasco V-660 spectrophotometer.

All reactions involving aromatic azides were carried out in the dark. **CAUTION!** Working with azide salts in the presence of halogenated solvents could lead to the formation of hazardous diazomethane.

After 1 month we have observed a slow decomposition of **1a–c** fluorogenic dyes even storing it under an inert atmosphere at −20 °C in the dark. Although the amount of the decomposition product is not significant it is advisable to purify it before usage by passing through a short plug of silica using CH_2Cl_2 as an eluent.

Synthesis of dyes

(*E*)-2-(4-Nitrostyryl)-1,3-benzothiazole (4a). 2-Methyl-1,3-benzothiazole (**2a**) (250 mg, 1.675 mmol, 1 eq.), 4-nitro-benzaldehyde (253 mg, 1.674 mmol, 1 eq.) and *p*-toluenesulfonic acid monohydrate (350 mg, 1.840 mmol, 1.1 eq.) were mixed in toluene (2 ml) in a rubber septum sealed vial. The reaction mixture was stirred at 110 °C for 18 h. Toluene was removed by evaporation *in vacuo* from the dark red suspension. Ethanol (6–8 ml) was added to the mixture and boiled for a few minutes. The suspension was then allowed to cool to r.t. and filtered. The product was washed few times with ethanol to give a yellow powder (408 mg, 86%). R_f = 0.47 (hexanes–EtOAc 5 : 1); mp >218 °C (decompose); IR (neat): ν_{max}/cm^{-1} 1517 and 1340 (NO_2); δ_H(600 MHz, DMSO-d_6) 8.28 (2 H, d, J = 8.5 Hz, Ar-H), 8.14 (1 H, d, J = 7.9 Hz, Ar-H), 8.07 (2 H, d, J = 8.5 Hz, Ar-H), 8.03 (1 H, d, J = 7.9 Hz, Ar-H), 7.88 (1 H, d, J = 16.1 Hz, CH═CH), 7.82 (1 H, d, J = 16.1 Hz, CH═CH), 7.55 (1 H, t, J = 7.6 Hz, Ar-H), 7.48 (1 H, t, J = 7.2 Hz, Ar-H); δ_C(150 MHz, DMSO-d_6) 165.5, 153.3, 147.2, 141.8, 134.7, 134.3, 128.6, 126.7, 125.9, 125.8, 123.9, 122.8, 122.3; HRMS (ESI) $[M + H]^+$ calcd for $[C_{15}H_{10}N_2O_2S + H]^+$: 283.0536, found: 283.0542.

(*E*)-2-(4-Aminostyryl)-1,3-benzothiazole (5a). $SnCl_2 \times 2H_2O$ (639 mg, 2.832 mmol, 4 eq.) in cc. HCl(aq.) (6 ml) was stirred for 5 minutes. (*E*)-2-(4-Nitrostyryl)-1,3-benzothiazole (**4a**) (200 mg, 0.7084 mmol, 1 eq.) was added to it in portions and the resulting mixture was stirred overnight at r.t. After all nitro compounds were consumed (followed by TLC) the reaction mixture was poured onto ice-water (50 ml). The pH was made basic with saturated NaOH solution and the resulting mixture was extracted with CH_2Cl_2 (3 × 20 ml). The combined organic phases were washed with brine (1 × 30 ml) and dried over $MgSO_4$. After filtering and evaporating the solvent a pale yellow solid was obtained (131 mg, 73%). R_f = 0.11 (hexanes–EtOAc 5 : 1); mp >178 °C (decompose); IR (neat) ν_{max}/cm^{-1} 3316 br and 1598 (NH_2); δ_H(250 MHz, $CDCl_3$) 7.96 (1 H, d, J = 8.1 Hz, Ar-H), 7.83 (1 H, d, J = 7.9 Hz, Ar-H), 7.44–7.38 (4 H, m, 3 × Ar-H, CH═CH), 7.33 (1 H, t, J = 7.5 Hz, Ar-H), 7.21 (1 H, d, J = 16.3 Hz, CH═CH), 6.68 (2 H, d, J = 8.0 Hz, Ar-H), 3.92 (1.6 H, brs, NH_2); δ_C(62.5 MHz, $CDCl_3$) 167.9, 153.9, 147.9, 138.0, 134.1, 129.0, 126.1, 125.8, 124.9, 122.5, 121.4, 118.2, 115.0; HRMS (ESI) $[M + H]^+$ calcd for $[C_{15}H_{12}N_2S + H]^+$: 253.0794, found: 253.0795.

(*E*)-2-(4-Azidostyryl)-1,3-benzothiazole (1a)

*Method A (from **5a**).* (*E*)-2-(4-Aminostyryl)-1,3-benzothiazole (**5a**) (100 mg, 0.3963 mmol, 1 eq.) was dissolved in a mixture of 2 ml cc. HCl(aq.), 2 ml water and 1 ml MeOH. To this solution was added an $NaNO_2$ solution (33 mg, 0.4783 mmol, 1.2 eq. in 200 µl water, +100 µl washing water) at 0 °C, dropwise. *Covering the reaction flask with aluminium foil is necessary from this point!* The temperature was kept at 0 °C, and after 10 minutes an NaN_3 solution (31 mg, 0.4768 mmol, 1.2 eq. in 200 µl water, +100 µl washing water) was added dropwise, slowly. After the addition, the mixture was allowed to warm to r.t. and stirred for a further 3 h. Next, the reaction mixture was poured onto ice-water (20–30 ml), extracted with CH_2Cl_2 (4 × 15 ml) and washed with brine (1 × 15 ml). After drying over $MgSO_4$ the drying agent was removed by filtration and the filtrate was concentrated *in vacuo*. The product was purified by column chromatography (SiO_2, hexanes–EtOAc = 10 : 1 → 7 : 1) to result in a pale yellow solid that was further washed with hexanes to obtain a 65 mg (59%) product. R_f = 0.62 (hexanes–EtOAc 5 : 1); mp >170 °C (decompose); IR (neat) ν_{max}/cm^{-1} 2115 (N_3); δ_H(600 MHz, $CDCl_3$) 7.99 (1 H, d, J = 7.7 Hz, Ar-H), 7.86 (1 H, d, J = 8.5 Hz, Ar-H), 7.56 (2 H, d, J = 8.5 Hz, Ar-H), 7.48 (1 H, d, J = 16.3 Hz, CH═CH), 7.47 (1 H, t, J = 8.5 Hz, Ar-H), 7.37 (1 H, t, J = 7.0 Hz, Ar-H), 7.34 (1 H, d, J = 16.3 Hz, CH═CH), 7.06 (2 H, d, J = 8.5 Hz, Ar-H); δ_C(62.5 MHz, $CDCl_3$) 166.7, 153.9, 141.0, 136.3, 134.4, 132.3, 128.8, 126.3, 125.3, 123.0, 121.8, 121.5, 119.5; HRMS (ESI) $[M + H]^+$ calcd for $[C_{15}H_{10}N_4S + H]^+$: 279.0699, found: 279.0695.

*Method B (from **7a**).* 1-(4-Azidophenyl)-2-(1,3-benzothiazol-2-yl)ethanol (**7a**) (263 mg, 0.8875 mmol) was stirred in dry toluene (7 ml) in the presence of 3 Å molecular sieves. After wrapping the flask with an aluminium foil the reaction mixture was heated to 70 °C. During warming the reactant was dissolved completely. Trifluoroacetic acid was added (2 drops) and the reaction mixture was stirred for 16 h. After cooling to

r.t. it was diluted with CH_2Cl_2 (8 ml) and the organic phase was washed with water (2 ml) and dried over $MgSO_4$. The mixture was then filtered and the solvent was evaporated. The residue was purified by column chromatography (SiO_2, hexanes–EtOAc = 10 : 1 → 5 : 1). The pale yellow residue (44 mg) was transferred onto a filter funnel and washed with hot hexanes (3–5 ml). A pale yellow powder was obtained (30 mg, 12%).

(*E*)-6-Methoxy-2-(4-nitrostyryl)-1,3-benzothiazole (4b). 2-Methyl-6-methoxy-1,3-benzothiazole (**2b**) (300 mg, 1.674 mmol, 1 eq.), 4-nitro-benzaldehyde (253 mg, 1.674 mmol, 1 eq.) and *p*-toluenesulfonic acid monohydrate (350 mg, 1.840 mmol, 1.1 eq.) were mixed in toluene (2 ml). After closing with a rubber septum the reaction mixture was heated to 110 °C and stirred for 18 h. Toluene was evaporated from the dark yellow suspension on a rotary evaporator. Ethanol (10 ml) was added and boiled for a few minutes, then cooled to r.t. and filtered. The filtered solid was washed with a little amount of ethanol to give an orange-yellow powder (129 mg, 25%). R_f = 0.36 (hexanes–EtOAc 5 : 1); mp >256 °C (decompose); IR (neat) ν_{max}/cm^{-1} 1506 and 1334 (NO_2), 1218 (C_{aryl}–O–C_{alkyl}); δ_H(600 MHz, DMSO-d_6) 8.27 (2 H, d, J = 8.9 Hz, Ar-H), 8.04 (2 H, d, J = 8.5 Hz, Ar-H), 7.91 (1 H, d, J = 8.9 Hz, Ar-H), 7.82 (1 H, d, J = 16.2 Hz, CH=CH), 7.72 (1 H, d, J = 2.7 Hz, Ar-H), 7.70 (1 H, d, J = 16.2 Hz, CH=CH), 7.14 (1 H, dd, J_1 = 8.9 Hz, J_2 = 2.5 Hz, Ar-H), 3.86 (3 H, s, CH_3); δ_C(150 MHz, DMSO-d_6) 165.8, 157.8, 147.1, 142.0, 136.0, 133.5, 128.4, 126.1, 123.4, 124.0, 119.6, 116.2, 104.7, 55.7; HRMS (ESI) $[M + H]^+$ calcd for $[C_{16}H_{12}N_2O_3S + H]^+$: 313.0641, found: 313.0643.

(*E*)-6-Methoxy-2-(4-aminostyryl)-1,3-benzothiazole (5b). $SnCl_2 \times 2H_2O$ (295 mg, 1.308 mmol, 4 eq.) in cc. HCl(aq.) (6 ml) was stirred for 5 minutes. (*E*)-6-Methoxy-2-(4-nitrostyryl)-1,3-benzothiazole (**4b**) (103 mg, 0.3298 mmol) was added to it in portions and the resulting mixture was stirred for 1 h at 45 °C. After cooling to r.t. the reaction mixture was poured onto ice-water (20 ml) and the pH was made basic using saturated NaOH solution. The mixture was extracted with CH_2Cl_2 (4 × 15 ml), and the combined organic phases were washed with brine (1 × 20 ml) and dried over $MgSO_4$. After filtration and removal of the solvent the residue was purified on a short column (SiO_2, CH_2Cl_2–MeOH = 10 : 0 → 10 : 1) to obtain the product as a pale yellow solid (89 mg, 96%). R_f = 0.07 (hexanes–EtOAc 5 : 1); mp >183 °C (decompose); IR (neat) ν_{max}/cm^{-1} 3316 br and 1622 (NH_2), 1218 (C_{aryl}–O–C_{alkyl}); δ_H(250 MHz, $CDCl_3$) 7.83 (1 H, d, J = 8.8 Hz, Ar-H), 7.38 (2 H, d, J = 8.4 Hz, Ar-H), 7.31–7.25 (2 H, m, CH=CH and Ar-H), 7.17 (1 H, d, J = 16.1 Hz, CH=CH), 7.04 (1 H, dd, J_1 = 9.0 Hz, J_2 = 2.5 Hz, Ar-H), 6.68 (2 H, d, J = 8.5 Hz, Ar-H), 3.89 (1.6 H, brs, NH_2), 3.88 (3 H, s, CH_3); δ_C(62.5 MHz, $CDCl_3$) 165.5, 157.6, 148.5, 147.7, 137.0, 135.5, 128.8, 126.0, 123.0, 118.4, 115.2, 115.1, 104.2, 55.8; HRMS (ESI) $[M + H]^+$ calcd for $[C_{16}H_{14}N_2OS + H]^+$: 283.0900, found: 283.0906.

(*E*)-6-Methoxy-2-(4-azidostyryl)-1,3-benzothiazole (1b)

*Method A (from **5b**).* (*E*)-6-Methoxy-2-(4-aminostyryl)-1,3-benzothiazole (**5b**) (77 mg, 0.2727 mmol, 1 eq.) was dissolved in a mixture of 1.5 ml cc. HCl(aq.), 1.5 ml water and 2 ml MeOH. To this solution was added $NaNO_2$ solution (23 mg, 0.3333 mmol, 1.2 eq. in 300 µl water, +100 µl washing water) at 0 °C, dropwise. *Covering the reaction flask with aluminium foil is necessary from this point!* The temperature was kept at 0 °C, and after 10 minutes an NaN_3 solution (21 mg, 0.3230 mmol, 1.2 eq. in 300 µl water, +100 µl washing water) was added dropwise. After the addition the mixture was allowed to warm to r.t. and stirred for a further 3 h. Next, the reaction mixture was poured onto ice-water (15–20 ml), extracted with CH_2Cl_2 (3 × 10 ml) and washed with brine (1 × 10 ml). The organic phase was dried over $MgSO_4$ and filtered. The solvent was evaporated on a rotary evaporator and the residue purified by column chromatography (SiO_2, CH_2Cl_2) to give a pale yellow solid that was transferred onto a filter funnel and washed with a little amount of hexanes (3–5 ml), and dried (54 mg, 64%). R_f = 0.50 (hexanes–EtOAc 5 : 1); mp >145 °C (melt and decompose); IR (neat) ν_{max}/cm^{-1} 2114 (N_3), 1266 (C_{aryl}–O–C_{alkyl}); δ_H(250 MHz, $CDCl_3$) 7.86 (1 H, d, J = 8.2 Hz, Ar-H), 7.54 (2 H, d, J = 8.2 Hz, Ar-H), 7.44–7.27 (3 H, m, CH=CH and 2 × Ar-H), 7.12–6.98 (3 H, m, Ar-H and CH=CH), 3.89 (3 H, s, C*H*$_3$); δ_C(62.5 MHz, $CDCl_3$) 164.3, 158.0, 148.4, 140.7, 135.8, 135.3, 132.5, 128.6, 123.5, 121.9, 119.5, 115.6, 104.1, 55.8; HRMS (ESI) $[M + H]^+$ calcd for $[C_{16}H_{12}N_4OS + H]^+$: 309.0805, found: 309.0807.

1-(4-Azidophenyl)-2-(1,3-benzothiazol-2-yl)ethanol (7a). 2-Methyl-1,3-benzothiazole (**2a**) (298 mg, 2 mmol, 1 eq.) and 4-azido-benzaldehyde (**6**) (294 mg, 2 mmol, 1 eq.) were dissolved in anhydrous dimethyl sulfoxide (6 ml). NaOMe (119 mg, 2.2 mmol, 1.1 eq.) was added and through septa the atmosphere was changed to nitrogen in the reaction flask and it was covered with aluminium foil. The stirring was continued for 20 h at r.t. (The reactants did not react completely). The dark reaction mixture was diluted with cold water (40 ml) and extracted with CH_2Cl_2 (3 × 50 ml) and the combined organic layers were washed with water (1 × 20 ml) and dried over $MgSO_4$. After filtration and evaporation the residue was purified by column chromatography (SiO_2, hexanes–EtOAc = 5 : 1 → 3 : 1). An orange solid was obtained (273 mg, 46%). The product was sufficiently pure and was used directly in the next step without further purification. R_f = 0.33 (hexanes–EtOAc 3 : 1); δ_H(250 MHz, $CDCl_3$) 8.01 (1 H, d, J = 8.2 Hz, Ar-H), 7.86 (1 H, d, J = 8.8 Hz, Ar-H), 7.45 (2 H, d, J = 8.8 Hz, Ar-H), 7.49 (1 H, t, J = 7.6 Hz, Ar-H), 7.39 (1 H, t, J = 7.5 Hz, Ar-H), 7.03 (2 H, d, J = 8.8 Hz, Ar-H), 5.29 (1 H, t, J = 6.0 Hz, C*H*-OH), 4.44 (0.9 H, br s, O*H*), 3.43 (2 H, d, J = 6.3 Hz, C*H*$_2$); δ_C(62.5 MHz, $CDCl_3$) 168.5, 152.7, 139.5, 134.6, 128.8, 127.3, 126.2, 125.2, 122.7, 121.5, 119.1, 72.1, 42.8.

(*E*)-6-Nitro-2-(4-azidostyryl)-1,3-benzothiazole (1c)

*Method B (from **7c**).* 1-(4-Azidophenyl)-2-(6-nitro-1,3-benzothiazol-2-yl)ethanol (**7c**) (231 mg, 0.6767 mmol) was stirred in dry toluene (5 ml) in the presence of 3 Å molecular sieves. After covering with aluminium foil the reaction vessel was warmed to 70 °C. Meanwhile, the reactant was dissolved completely. Trifluoroacetic acid was added (3 drops) and the reaction mixture was stirred for 7 h. During the reaction the product precipitated as an orange powder. After cooling to 3–5 °C (in fridge) the precipitate was filtered and washed with

hot hexanes (2–3 ml). A yellow powder was obtained (82 mg, 37%). R_f = 0.48 (hexanes–EtOAc 3 : 1); mp >178 °C (decompose); IR (neat) ν_{max}/cm^{-1} 2133 (N_3), 1510 and 1340 (NO_2); δ_H(250 MHz, $CDCl_3$) 8.79 (1 H, d, J = 1.9 Hz, Ar-H), 8.35 (1 H, dd, J_1 = 8.8 Hz, J_2 = 2.5 Hz, Ar-H), 8.05 (1 H, d, J = 8.8 Hz, Ar-H), 7.61 (1 H, d, J = 15.8 Hz, CH=CH), 7.60 (2 H, d, J = 9.5 Hz, Ar-H), 7.35 (1 H, d, J = 16.4 Hz, CH=CH), 7.09 (2 H, d, J = 8.8 Hz, Ar-H); δ_C(62.5 MHz, $CDCl_3$) 172.3, 157.7, 144.9, 141.9, 139.1, 134.7, 131.5, 129.3, 122.9, 122.0, 120.7, 119.7, 118.1; HRMS (ESI) $[M + H]^+$ calcd for $[C_{15}H_9N_5O_2S + H]^+$: 324.0555; found: 324.0557.

1-(4-Azidophenyl)-2-(6-nitro-1,3-benzothiazol-2-yl)ethanol (7c). 6-Nitro-2-methyl-1,3-benzothiazole (**2c**) (300 mg, 1.545 mmol, 1 eq.) and 4-azido-benzaldehyde (**6**) (250 mg, 1.799 mmol, 1.2 eq.) were dissolved in anhydrous dimethyl sulfoxide (9 ml). NaOMe (100 mg, 1.851 mmol, 1.2 eq.) was added under a nitrogen atmosphere and the flask was covered with aluminium foil. The stirring was continued for 17 h at r.t. The dark reaction mixture was diluted with cold water (90 ml) and extracted with CH_2Cl_2 (3 × 60 ml). The combined organic phases were washed with water (1 × 70 ml), brine (1 × 70 ml) and dried over $MgSO_4$. After filtration the solvent was removed *in vacuo* and the residue was purified by column chromatography (SiO_2, hexanes–EtOAc = 5 : 1 → 2 : 1). An orange-yellow viscous compound was obtained (231 mg, 44%). The product was sufficiently pure and was used directly in the next step without further purification. R_f = 0.15 (hexanes–EtOAc 3 : 1); δ_H(250 MHz, $CDCl_3$) 8.75 (1 H, d, J = 2.2 Hz, Ar-H), 8.32 (1 H, dd, J_1 = 8.9 Hz, J_2 = 2.3 Hz, Ar-H), 8.04 (1 H, d, J = 9.0 Hz, Ar-H), 7.40 (2 H, d, J = 8.4 Hz, Ar-H), 7.00 (2 H, d, J = 8.5 Hz, Ar-H), 5.28 (1 H, t, J = 6.2 Hz, C*H*-OH), 4.01 (0.7 H, br s, O*H*), 3.49 (2 H, d, J = 6.0 Hz, CH_2); δ_C(62.5 MHz, $CDCl_3$) 174.7 and 173.3, 156.9 and 156.2, 144.8 and 144.6, 139.6 and 139.1, 135.8 and 135.2, 127.15 and 127.13 (CH), 122.7 and 122.4 (CH), 121.5 and 121.4 (CH), 119.1 (CH), 118.0 and 117.8 (CH), 71.8 (CH), 43.5 ppm (CH_2). Duplication of peaks is most probably due to the chelate effect between OH and N=. The orders of the carbons were determined by DEPT135 measurement.

Synthesis of click conjugates

General method. The azides (**1a–c**) (1 eq.) and *N*-(prop-2-ynyl)pivalamide[18] (**8**) (1.5 eq.) were stirred in CH_2Cl_2 (1 ml, stabilized with amylene) at r.t. in the presence of triethylamine (4 µl) and a pinch of $Cu(PPh_3)_2NO_3$ catalyst[10] for 8 h. The resulting suspension was diluted with hexanes (4 ml), filtered and the products were washed with a little amount of CH_2Cl_2 (1–1.5 ml) and hexanes (5 ml).

Click compound 9a. It was obtained from (*E*)-2-(4-azidostyryl)-1,3-benzothiazole (**1a**) (15.0 mg, 0.0538 mmol) and *N*-(prop-2-ynyl)pivalamide (**8**) (11.3 mg, 0.0812 mmol). White-pale yellow fibrous solid (17 mg, 76%). R_f = 0.73 (CH_2Cl_2–MeOH 9 : 1); mp >258 °C (decompose); IR (neat) ν_{max}/cm^{-1} 3311 br (aromatic ring) 1627 and 1541 (CONHR); δ_H(600 MHz, DMSO-d_6) 8.59 (1 H, s, triazole-H), 8.12 (1 H, d, J = 8.2 Hz, Ar-H), 8.07 (1 H, t, J = 5.6 Hz, NH), 8.03–7.98 (5 H, m, 5 × Ar-H), 7.76 (1 H, d, J = 16.4 Hz, CH=CH), 7.73 (1 H, d, J = 16.4 Hz, CH=CH), 7.54 (1 H, t, J = 8.0 Hz, Ar-H), 7.46 (1 H, t, J = 7.6 Hz, Ar-H), 4.39 (2 H, d, J = 5.9 Hz, CH_2), 1.13 (9 H, s, CH_3); δ_C(150 MHz, DMSO-d_6) 177.4, 166.1, 153.4, 146.8, 136.8, 135.9, 135.2, 134.1, 129.0, 126.5, 125.5, 122.7, 122.5, 122.2, 120.5, 120.0, 37.9, 34.5, 27.3; HRMS (ESI) $[M + H]^+$ calcd for $[C_{23}H_{23}N_5OS + H]^+$: 418.1696, found: 418.1701.

Click compound 9b. It was obtained from (*E*)-6-methoxy-2-(4-azidostyryl)-1,3-benzothiazole (**1b**) (15.0 mg, 0.04864 mmol) and *N*-(prop-2-ynyl)pivalamide (**8**) (10.2 mg, 0.0733 mmol). White-pale yellow fibrous solid (13 mg, 60%). R_f = 0.68 (CH_2Cl_2–MeOH 9 : 1); mp >214 °C (decompose); IR (neat) ν_{max}/cm^{-1} 3331 br (aromatic ring), 1624 and 1536 (CONHR).1224 (C_{aryl}–O–C_{alkyl}); δ_H(600 MHz, DMSO-d_6) 8.58 (1 H, s, triazole-H), 8.07 (1 H, t, J = 5.5 Hz, NH), 7.98 (4 H, s, Ar-H), 7.88 (1 H, d, J = 9.0 Hz, Ar-H), 7.71–7.65 (2 H, m, CH=CH and Ar-H), 7.64 (1 H, d, J = 16.2 Hz, CH=CH), 7.12 (1 H, dd, J_1 = 9.0 Hz, J_2 = 1.7 Hz, Ar-H), 4.39 (2 H, d, J = 5.5 Hz, CH_2), 3.86 (3 H, s, O–CH_3), 1.13 (9 H, s, CH_3); δ_C(150 MHz, DMSO-d_6) 177.4, 163.5, 157.6, 147.8, 146.7, 136.6, 135.6, 135.4, 134.7, 128.8, 123.1, 122.9, 120.5, 120.0, 115.8, 104.7, 55.7, 37.9, 34.5, 27.3; HRMS (ESI) $[M + H]^+$ calcd for $[C_{24}H_{25}N_5O_2S + H]^+$: 448.1802, found: 448.1802.

Click compound 9c. It was obtained from (*E*)-6-nitro-2-(4-azidostyryl)-1,3-benzothiazole (**1c**) (15 mg, 0.04639 mmol) and *N*-(prop-2-ynyl)pivalamide (**8**) (9.7 mg, 0.0697 mmol). Yellow powder (14 mg, 65%). R_f = 0.70 (CH_2Cl_2–MeOH 9 : 1); mp >240 °C (decompose); IR (neat) ν_{max}/cm^{-1} 3293 (aromatic ring), 1516 and 1336 (NO_2), 1628 (CONHR); δ_H(600 MHz, DMSO-d_6) 9.20 (1 H, d, J = 2.3 Hz, Ar-H), 8.60 (1 H, s, triazole-H), 8.34 (1 H, dd, J_1 = 8.8 Hz, J_2 = 2.3 Hz, Ar-H), 8.16 (1 H, d, J = 9.4 Hz, Ar-H), 8.08 (1 H, t, J = 5.6 Hz, NH), 8.05 (2 H, d, J = 8.8 Hz, Ar-H), 8.02 (2 H, d, J = 8.8 Hz, Ar-H), 7.92 (1 H, d, J = 15.8 Hz, CH=CH), 7.82 (1 H, d, J = 16.4 Hz, CH=CH), 4.39 (2 H, d, J = 5.9 Hz, CH_2), 1.13 (9 H, s, CH_3); δ_C(150 MHz, DMSO-d_6) 177.4, 172.5, 157.2, 146.8, 144.2, 138.2, 137.2, 134.8, 129.5, 122.7, 122.2, 121.9, 120.6, 120.0, 119.3, 37.9, 34.4, 27.3; HRMS (ESI) $[M + H]^+$ calcd for $[C_{23}H_{22}N_6O_3S + H]^+$: 463.1547, found: 463.1553.

Model reactions with CyO-peptide

The reaction mixture contained 1×10^{-4} M azido-dye (**1b**, **1c**) and 2×10^{-4} M CyO-peptide in a 2 ml phosphate buffered solution. For fluorescence measurements aliquots were drawn from the reaction mixture: a 25 µl reaction mixture and a 2475 µl phosphate buffer were mixed (final concentration 1×10^{-6} M for the starting amount of dye) and emission was monitored at emission maxima using 355 nm excitation.

1b + CyO-pep. 650 µl 3.24×10^{-4} M **1b** (DMSO solution), 400 µl 1.00×10^{-3} M CyO-pep and 950 µl phosphate buffer (pH 7.20) incubated at 37 °C, covered with aluminium foil.

The control experiment contained 650 µl 3.24×10^{-4} M **1b** (DMSO solution) and 1350 µl phosphate buffer (pH 7.20) and incubated at the same temperature.

1c + CyO-pep. 497 µl 4.02×10^{-4} M **1b** (DMSO solution), 400 µl 1.00×10^{-3} M CyO-pep and 1103 µl phosphate buffer

(pH 7.20) were incubated at 37 °C, covered with aluminium foil.

The control experiment contained 497 μl 4.021×10^{-4} M **1b** (DMSO solution) and 1503 μl phosphate buffer (pH 7.20) and incubated at the same temperature.

Live cell labeling and lysate analysis of cyclooctyne expressing *E. coli*

Top 10 *E. coli* cells containing pEvol $PylRS^{AF}$ and pBAD plasmids for expressing GFP^{Y39TAG} or GFP^{WT} were grown in the presence of ampicillin and chloramphenicol in a Terrific broth medium. GFP^{Y39TAG} was grown in the presence ($GFP^{Y39TAG+SCO}$) and absence of SCO ($GFP^{Y39TAG-SCO}$) and GFP^{WT} was grown also in the presence of SCO.[2a,b] Cells were induced with arabinose at OD 0.4 and allowed to grow overnight. After harvesting, the cells were resuspended in 1× phosphate buffered saline (PBS, pH 7.4) and the OD was adjusted to ~1.7. A total volume of 1.5 ml of this suspension was used in further steps. The cells were centrifuged and washed 3 times with PBS. Pellets were afterwards resuspended in 1 ml PBS and incubated with 500 μM compounds **1b**, **1c** (both 50 mM stock in DMSO) or 50 μM of TAMRA-azide (40 mM stock in DMSO) at 37 °C in the dark shaking for 4.5 h. After labeling, the cells were centrifuged and pellets were washed rigorously with PBS containing 5% DMSO. Subsequently samples were lysed and loaded onto an SDS PAGE gel for whole cell lysate analysis. The gel was analysed for fluorescence by exciting the samples in the UV-range (365 nm) and detecting the emission with an ethidium bromide filter setting on a commercially available gel documentation system (Alpha Innotech, CA). Afterwards the gel was stained with Coomassie.

Conclusion

In conclusion, we have developed synthetic procedures for the construction of fluorogenic tags. In addition, by using theoretical chemical calculations we are able to predict and screen for potential fluorogenic azides that are worth to be synthesized. We have selected and synthesized three new fluorogenic and bioorthogonally applicable dyes, **1a–c**. In aqueous media the azides **1a–c** are virtually non-fluorescent. Although "clicked" triazole derivative **9a** exhibits moderately increased emission intensity, **9b** and **9c** show intense fluorescence. Photophysical studies have justified **1b** and **1c** as remarkably suitable for bioorthogonal tagging schemes. The performance of these two fluorogenic tags was tested in the fluorescence tagging of a peptide sequence by means of a strain-promoted azide–alkyne cycloaddition reaction. Both tags exhibited excellent performance. Furthermore, the applicability of these fluorogenic tags was further demonstrated in *in vivo* cell labeling experiments. Analysis of the gel-electrophoresis chromatograms of the cell lysates revealed that both tags can be used in background fluorescence free bioorthogonal tagging schemes.

The synthetic approach and the theoretical screen of possible fluorogenic tags will allow the generation of libraries of such tags. Fast screening of these libraries greatly facilitates the selection of fluorogenic tags for certain needs (*e.g.* excitation and emission wavelengths). Work aiming at the synthesis of such designed libraries is underway in our laboratory and results will be reported in due course. Further aims are to fine tune the photophysical properties of such tags and generate fluorogenic azides that are excitable in the red-far-red, near infrared region as these regimes are more suitable for biological tagging and detection schemes.

Acknowledgements

P. K. acknowledges the support of the Hungarian Academy of Sciences for the János Bolyai Fellowship (BO/00148/11/7). Financial support of the Hungarian Scientific Research Fund (OTKA), Grant No. K100134 is also greatly appreciated. M. K. acknowledges the financial support by the European Research Council (ERC) under the European Community's Seventh Framework Programme (FP7/2007–2013), ERC Grant Agreement No. 200639. I. N. acknowledges support by an EMBO Long-Term Fellowship and E. A. L. funding of the DFG Emmy Noether and SPP1623 program.

Notes and references

1 (*a*) J. C. Jewett and C. R. Bertozzi, *Chem. Soc. Rev.*, 2010, **39**, 1272; (*b*) C. R. Becer, R. Hoogenboom and U. Schubert, *Angew. Chem., Int. Ed.*, 2009, **48**, 4900; (*c*) K. V. Reyna and Q. Lin, *Chem. Commun.*, 2010, **46**, 1589; (*d*) K. E. Beatty, *Mol. BioSyst.*, 2011, **7**, 2360; (*e*) M. F. Debets, S. S. van Berkel, J. Dommerholt, A. T. J. Dirks, F. P. J. T. Rutjes and F. L. van Delft, *Acc. Chem. Res.*, 2011, **44**, 805; (*f*) B. R. Varga, M. Kállay, K. Hegyi, Sz. Béni and P. Kele, *Chem.–Eur. J.*, 2012, **18**, 822.

2 (*a*) T. Plass, S. Milles, C. Koehler, C. Schultz and E. A. Lemke, *Angew. Chem., Int. Ed.*, 2011, **50**, 3878; (*b*) T. Plass, S. Milles, C. Koehler, J. Szymański, R. Mueller, M. Wießler, C. Schultz and E. A. Lemke, *Angew. Chem., Int. Ed.*, 2012, **51**, 4166; (*c*) S. J. Luchansky and C. R. Bertozzi, *ChemBioChem*, 2004, **5**, 1706; (*d*) N. J. Agard, J. M. Baskin, J. A. Prescher, A. Lo and C. R. Bertozzi, *ACS Chem. Biol.*, 2006, **1**, 644; (*e*) K. E. Beatty, F. Xie, Q. Wang and D. A. Tirrell, *J. Am. Chem. Soc.*, 2005, **127**, 14150; (*f*) A. Borrmann, S. Milles, T. Plass, J. Dommerholt, J. M. M. Verkade, M. Wießler, C. Schultz, J. C. M. van Hest, F. L. van Delft and E. A. Lemke, *ChemBioChem*, 2012, **13**, 2094; (*g*) G. Charbon, E. Brustad, K. A. Scott, J. Wang, A. Løebner-Olesen, P. G. Schultz, C. Jacobs-Wagner and E. Chapman, *ChemBioChem*, 2011, **12**, 1818; (*h*) A. R. Katritzky and T. Narindoshvili, *Org. Biomol. Chem.*, 2009, **7**, 627.

3 (*a*) M. S. T. Gonçalves, *Chem. Rev.*, 2009, **109**, 190; (*b*) S. Chen, X. Li and H. Ma, *ChemBioChem*, 2009, **10**, 1200; (*c*) J. H. Lee, J.-H. So, J. H. Jeon, E. B. Choi, Y.-R. Lee,

Y.-t. Chang, C.-H. Kim, M. A. Bae and J. H. Ahn, *Chem. Commun.*, 2011, **47**, 7500; (*d*) T. Ehrenschwender, B. R. Varga, P. Kele and H.-A. Wagenknecht, *Chem.–Asian J.*, 2010, **5**, 1761; (*e*) M. Sato, Y. Ito, N. Arima, M. Baba, M. Sobel, M. Wakao and Y. Suda, *J. Biochem.*, 2009, **146**, 33; (*f*) P. Kele, X. Li, M. Link, K. Nagy, A. Herner, K. Lőrincz, Sz. Béni and O. S. Wolfbeis, *Org. Biomol. Chem.*, 2009, **7**, 3486.

4 (*a*) A. Nadler and C. Schultz, *Angew. Chem., Int. Ed.*, 2013, **52**, 2408–2410; (*b*) C. Le Droumaguet, C. Wang and Q. Wang, *Chem. Soc. Rev.*, 2010, **39**, 1233; (*c*) K. Sivakumar, F. Xie, B. M. Cash, S. Long, H. N. Barnhill and Q. Wang, *Org. Lett.*, 2004, **6**, 4603; (*d*) J. Qi, M.-S. Han, Y.-C. Chang and C.-H. Tung, *Bioconjugate Chem.*, 2011, **22**, 1758; (*e*) G. Lukinavičius and K. Johnsson, *Curr. Opin. Chem. Biol.*, 2011, **15**, 768; (*f*) J. C. Jewett and C. R. Bertozzi, *Org. Lett.*, 2011, **13**, 5937.

5 P. Shieh, M. J. Hangauer and C. R. Bertozzi, *J. Am. Chem. Soc.*, 2012, **134**, 17428.

6 (*a*) M. F. Debets, Ch. W. J. van der Doelen, F. P. J. T. Rutjes and F. L. van Delft, *ChemBioChem*, 2010, **11**, 1168; (*b*) J. M. Baskin and C. R. Bertozzi, *Aldrichimica. Acta*, 2010, **43**, 15–23.

7 (*a*) M. Meldal and C. W. Tornøe, *Chem. Rev.*, 2008, **108**, 2952; (*b*) P. V. Chang, J. A. Prescher, E. M. Sletten, J. M. Baskin, I. A. Miller, N. J. Agard, A. Lo and C. R. Bertozzi, *Proc. Natl. Acad. Sci. U. S. A.*, 2010, **107**, 1821; (*c*) C. I. Schilling, N. Jung, M. Biskup, U. Schepers and S. Bräse, *Chem. Soc. Rev.*, 2011, **40**, 4840.

8 (*a*) Z. Zhou and C. J. Fahrni, *J. Am. Chem. Soc.*, 2004, **126**, 8862; (*b*) L. Yongjun, L. Ying, K. Xianghe, X. Min and L. Chengbu, *Theor. Exp. Chem.*, 2000, **36**, 303.

9 (*a*) G. B. Cserép, K. N. Enyedi, A. Demeter, G. Mező and P. Kele, *Chem.–Asian J.*, 2013, **8**, 494; (*b*) K. Nagy, E. Orbán, Sz. Bősze and P. Kele, *Chem.–Asian J.*, 2010, **5**, 773.

10 (*a*) C. G. Bates, P. Saejueng, J. M. Murphy and D. Venkataraman, *Org. Lett.*, 2002, **4**, 4727; (*b*) Zs. Gonda and Z. Novák, *Dalton Trans.*, 2010, **39**, 726.

11 D. F. Eaton, *Pure Appl. Chem.*, 1988, **60**, 1107.

12 M. J. Frisch, G. W. Trucks, H. B. Schlegel, G. E. Scuseria, M. A. Robb, J. R. Cheeseman, G. Scalmani, V. Barone, B. Mennucci, G. A. Petersson, H. Nakatsuji, M. Caricato, X. Li, H. P. Hratchian, A. F. Izmaylov, J. Bloino, G. Zheng, J. L. Sonnenberg, M. Hada, M. Ehara, K. Toyota, R. Fukuda, J. Hasegawa, M. Ishida, T. Nakajima, Y. Honda, O. Kitao, H. Nakai, T. Vreven, J. A. Montgomery Jr., J. E. Peralta, F. Ogliaro, M. Bearpark, J. J. Heyd, E. Brothers, K. N. Kudin, V. N. Staroverov, R. Kobayashi, J. Normand, K. Raghavachari, A. Rendell, J. C. Burant, S. S. Iyengar, J. Tomasi, M. Cossi, N. Rega, J. M. Millam, M. Klene, J. E. Knox, J. B. Cross, V. Bakken, C. Adamo, J. Jaramillo, R. Gomperts, R. E. Stratmann, O. Yazyev, A. J. Austin, R. Cammi, C. Pomelli, J. W. Ochterski, R. L. Martin, K. Morokuma, V. G. Zakrzewski, G. A. Voth, P. Salvador, J. J. Dannenberg, S. Dapprich, A. D. Daniels, Ö. Farkas, J. B. Foresman, J. V. Ortiz, J. Cioslowski and D. J. Fox, *GAUSSIAN 09 (Revision B.01)*, Gaussian, Inc., Wallingford CT, 2009.

13 J. P. Perdew, K. Burke and M. Ernzerhof, *Phys. Rev. Lett.*, 1996, **77**, 3865; Erratum: 1997, 78, 1396.

14 C. Adamo and V. Barone, *J. Chem. Phys.*, 1999, **110**, 6158.

15 S. Miertuš, E. Scrocco and J. Tomasi, *Chem. Phys.*, 1981, **55**, 117.

16 R. E. Stratmann, G. E. Scuseria and M. J. Frisch, *J. Chem. Phys.*, 1998, **109**, 8218.

17 P. Kele, G. Mező, D. Achatz and O. S. Wolfbeis, *Angew. Chem., Int. Ed.*, 2009, **48**, 344.

18 N. Willand, M. Desroses, P. Toto, B. Dirie, Z. Lens, V. Villeret, P. Rucktooa, C. Locht, A. Baulard and B. Deprez, *ACS Chem. Biol.*, 2010, **5**, 1007.

